

## Dynamics of atomic pairs in a Lennard-Jones fluid: Mean relative displacement analysis

Ten-Ming Wu and S. L. Chang

*Institute of Physics, National Chiao-Tung University, HsinChu, Taiwan 300, Republic of China*

(Received 28 July 1998)

We have analyzed the dynamics of atomic pairs in a simple fluid in terms of the mean relative displacement of two atoms with a given initial separation. The short-time expansion of the mean relative displacement has been derived exactly beyond the constant acceleration approximation (CAA) (up to the  $t^4$  order). For a Lennard-Jones fluid, the mean relative displacements calculated by either the CAA or the  $t^4$ -order approximation have been compared with the results obtained from a molecular-dynamics simulation. Through studying the relative motions of atomic pairs with different initial separations, we give a physical picture of the dynamics of neighboring atoms beyond the CAA. [S1063-651X(99)08603-1]

PACS number(s): 61.20.Lc, 82.20.Db, 61.20.Ja, 61.20.Ne

### I. INTRODUCTION

Many intermolecular spectroscopies in fluids are essentially related to the relative motions of particles. A recent example is the time-resolved transient fluorescence used to study the short-time dynamics of solvation at a molecular level [1–4]. For a probe molecule dissolved in a fluid, the transition frequency between the ground and excited states is affected by the difference of the solute-solvent interactions corresponding to the two electronic states, and also fluctuates due to the solvent motions relative to the solute [5,6]. The dynamics of these relative motions has strong effects on the autocorrelation function of the transition-frequency fluctuation, which is, within the linear response approximation, equivalent to the solvent response function measured by the Stokes shift of the transient fluorescence [3,4].

Using a molecular-dynamics (MD) simulation, Saven and Skinner [7] presented the transition frequency autocorrelation function of an atomic solvation model, in which one atomic solute is dissolved in a low-density, high-temperature Lennard-Jones (LJ) solvent fluid (with equal masses of all particles). In their simulated results, the transition frequency autocorrelation function, after being normalized, has a small bump arising at the time scale right after the rapid Gaussian decay, which is due to the ballistic motions of particles. They interpreted the occurrence of the bump as due to the vibrational motion of the solvent particles caged in the first shell around the solute. Their interpretation is based on the general concept of the potential of mean force [8]. However, it was concluded that the effects of the potential of the mean force upon the dynamics of pairs in an atomic fluid were significant only in the short-time regime [9,10].

In this well studied model [7,11,12], the interaction between particles in the ground state is described by a LJ potential, and the interaction between an excited solute and a solvent particle is by another LJ potential which has the same diameter, but a well depth deeper than the ground-state value. Thus the well depth of the excited-state solute-solvent LJ potential serves as the only tunable parameter in their model. However, due to this special model, the normalized transition frequency autocorrelation function is independent of this parameter. It is easier to study the dynamical effects

of particle relative motions on this autocorrelation function in a limiting case through the MD simulation, in which the model system has the same conditions as studied, but the well depth of the excited-state potential is infinitesimally close to the ground-state value. In such a limiting case, the dynamics of the model system is virtually identical to that of a pure simple LJ fluid. Therefore, with this motivation, we think it is worth investigating the relative motions of atomic pairs in a simple fluid from a short-time regime up to a time scale beyond the ballistic motion of individual particle.

Usually, the relative motions of atomic pairs in a simple fluid are described in terms of the time-dependent distribution function  $G_2(\mathbf{r}, \mathbf{r}'; t)$ , which is the conditional probability of finding a pair of atoms with separation vector  $\mathbf{r}'$  at time  $t$ , given that they were separated by  $\mathbf{r}$  at  $t=0$  [13,14]. The quantities usually presented and analyzed were the moments of this distribution [11–14]. In this paper, we suggest that the mean relative displacement  $\mathbf{U}(\mathbf{r}, t)$  of an atomic pair at time  $t$ , given that its initial separation vector was  $\mathbf{r}$ , is an effective quantity to manifest the dynamical and structural effects of the fluid on the relative motion of an atomic pair, especially for those nearest-neighbor pairs. The mean relative displacement, which describes the average center of the  $G_2$  distribution at time  $t$ , is one of the moments of this distribution, and is given by the equation

$$\mathbf{U}(\mathbf{r}, t) = \int d\mathbf{r}' G_2(\mathbf{r}, \mathbf{r}'; t) (\mathbf{r}' - \mathbf{r}). \quad (1)$$

In an uniform simple fluid, the relative motion of an atomic pair is anisotropic due to the initially specified separation of the two atoms, including both their relative distance and direction. Thus the mean relative displacement  $\mathbf{U}(\mathbf{r}, t)$  may be decomposed into two components  $U^{\parallel}(r, t)$  and  $U^{\perp}(r, t)$ , which are parallel and perpendicular to the initial separation vector  $\mathbf{r}$ , respectively, and depend only on  $r$ . For two atoms with a very large initial separation, these two components are certainly zero at all times, since the interaction between the two atoms is so small that each atom can be thought to be free from the other. As the initial separation of the two atoms is of the order of the mean nearest-neighbor distance of the fluid,  $U^{\parallel}(r, t)$  is no longer zero, since the two atoms interact directly and through the medium; however,

$U^\perp(r, t)$  is still zero at all times. Therefore, by analyzing the parallel components of the mean relative displacements of the atomic pairs, we may obtain information about the effects of the fluid structures on the relative motions of neighboring atoms.

In the gas phase, the relative motion of a pair is essentially determined by the direct potential  $\phi(r)$  between the two atoms. In a dense simple fluid, rather than the direct potential, the relative motion of a pair is actually determined by the averaged force between the two atoms, which includes both the direct force and the indirect forces intermediate through the remaining atoms in the fluid. The overall averaged force between two atoms in a fluid is given by the gradient of the potential of mean force  $w(r) \equiv -k_B T \ln g(r)$ , where  $g(r)$  is the radial distribution function of the fluid. In the low density limit,  $w(r)$  reduces to  $\phi(r)$ . The short-time dynamics of atomic pairs in a fluid can be well described by the constant acceleration approximation (CAA), which was first introduced by Oppenheim and Bloom in the theory of nuclear spin relaxation in fluids [15]. In the CAA, the forces between atoms in a fluid are independent of time, and thus the motions of particles are assumed to be ballistic.  $\mathbf{U}(\mathbf{r}, t)$  is, therefore, approximated to be  $-\frac{1}{2}t^2 \nabla w(r)/2\mu$ , with  $\mu$  to be the reduced mass of a pair. The mean relative displacement of a pair in the CAA is just the leading term of the short-time expansion of  $\mathbf{U}(\mathbf{r}, t)$ .

Recently, there has been great interest in analyzing the short-time dynamics of liquids in terms of instantaneous normal modes (INM's) [16–18]. In the INM approach, the forces between particles are approximated beyond the CAA by including the Hessian matrix of the total interaction of the system. Therefore, the dynamics of a liquid in the INM approximation includes some collective motions, rather than the ballistic motions of individual particles. In terms of INM's, the particle displacements from an instantaneous configuration are correct to  $t^2$ ; the velocity autocorrelation function of a particle is correct to  $t^4$ .

In the same spirit of the INM approach, in this paper we expand the particle displacements from a configuration up to the  $t^4$  order by solving the equations of motion with the iterating method. Instead of paying attention to the motions of all particles as in the INM approach, we focus only on the relative displacement of a single pair. After making an ensemble average, we obtain exactly the expansion of the mean relative displacement of a pair up to the  $t^4$  order. The derivation is given in Sec. II. In Sec. III, for a LJ fluid, the mean relative displacements of atomic pairs calculated in either the CAA or the  $t^4$ -order approximation are compared with the results obtained from MD simulation. By comparing the mean relative displacements of two groups of atomic pairs with an initial separation of one group at  $r_{\max}$  and initial separations of the other group at less than  $r_{\max}$ , where  $r_{\max}$  is the distance corresponding to the first maximum of  $g(r)$ , we show the dynamical and structural effects of the fluid on the relative motions of neighboring atoms. Our conclusion is given in Sec. IV.

## II. MEAN RELATIVE DISPLACEMENT

Consider a system of  $N$  particles each having a mass  $m$ , interacting via the pair potential  $\phi(r)$ . With the initial separa-

tion  $\mathbf{r}_{21} \equiv \mathbf{r}_2 - \mathbf{r}_1$  [ $\mathbf{r}_i \equiv \mathbf{r}_i(0)$ ] of a pair, indexed with 1 and 2, and their relative displacement  $\mathbf{u}_{21}(t) \equiv \mathbf{u}_2(t) - \mathbf{u}_1(t)$  [ $\mathbf{u}_i(t) \equiv \mathbf{r}_i(t) - \mathbf{r}_i$ ] at time  $t$ , we define the mean relative displacement of an atomic pair as

$$\mathbf{U}(\mathbf{r}, t) = \frac{\langle \delta(\mathbf{r} - \mathbf{r}_{21}) \mathbf{u}_{21}(t) \rangle}{\langle \delta(\mathbf{r} - \mathbf{r}_{21}) \rangle}, \quad (2)$$

where the angular brackets denote an equilibrium ensemble average. Since the system is in thermal equilibrium,  $\langle \delta(\mathbf{r} - \mathbf{r}_{21}) \rangle = g(r)/V$ , where  $V$  is the volume of the system.

From the equations of motion and the details given in the Appendix, the displacement  $\mathbf{u}_i(t)$  can be expanded into a time series. Up to the  $t^4$  order,

$$\mathbf{u}_i(t) = \mathbf{v}_i t + \frac{t^2}{2!m} \mathbf{F}_i - \frac{t^3}{3!m} \sum_j \mathbf{K}_{ij} \cdot \mathbf{v}_j - \frac{t^4}{4!m} \sum_{j,k} \left( \frac{1}{m} \mathbf{K}_{ij} \cdot \mathbf{F}_j + \mathbf{v}_j \cdot \mathbf{L}_{ijk} \cdot \mathbf{v}_k \right) + \dots, \quad (3)$$

$$\mathbf{F}_i \equiv -\nabla_i V(\mathbf{R})|_{\mathbf{R}=\mathbf{R}_0}, \quad (4)$$

$$\mathbf{K}_{ij} \equiv \nabla_i \nabla_j V(\mathbf{R})|_{\mathbf{R}=\mathbf{R}_0}, \quad (5)$$

$$\mathbf{L}_{ijk} \equiv \nabla_i \nabla_j \nabla_k V(\mathbf{R})|_{\mathbf{R}=\mathbf{R}_0}, \quad (6)$$

where  $\mathbf{v}_i$  is the initial velocity of the  $i$ th particle, and  $\mathbf{F}_i$  is the total force on the  $i$ th particle in the initial configuration  $\mathbf{R}_0$ .  $\mathbf{K}_{ij}$  and  $\mathbf{L}_{ijk}$ , respectively, are the second- and third-order expansion coefficients of the total potential  $V(\mathbf{R})$  of the system in the initial configuration  $\mathbf{R}_0$ .  $\mathbf{K}_{ij}$ , defined in Ref. [18], is actually a three-dimensional matrix. With a total potential  $V$  assumed to be a pairwise summation of the pair potential  $\phi(r)$ ,

$$\mathbf{K}_{ij} = \begin{cases} -\mathbf{t}(\mathbf{r}_{ij}) & \text{for } i \neq j \\ \sum_{l \neq j} \mathbf{t}(\mathbf{r}_{lj}) & \text{for } i = j, \end{cases} \quad (7)$$

$$\mathbf{t}(\mathbf{r}) = \frac{\phi'(r)}{r} \mathbf{I}_3 + \left( \phi''(r) - \frac{\phi'(r)}{r} \right) \hat{\mathbf{r}} \hat{\mathbf{r}}, \quad (8)$$

where  $\phi'(r)$  and  $\phi''(r)$  denote the first and second derivatives of the pair potential  $\phi(r)$  with respect to  $r$ ,  $\hat{\mathbf{r}}$  is the unit vector along  $\mathbf{r}$ , and  $\mathbf{I}_3$  is the three-dimensional unit matrix. Thus the  $\mathbf{K}_{ij}$  matrices obey the following sum rule:

$$\sum_{i=1}^N \mathbf{K}_{ij} = \sum_{j=1}^N \mathbf{K}_{ij} = 0. \quad (9)$$

The sum rule is proof that the net force on the center of mass of the system is zero.

After substituting the expanded series of particle displacements given in Eq. (3) into Eq. (2), and averaging out the initial velocities, we obtain a short-time expansion of the mean relative displacement, which contains only even powers of time. Up to  $t^4$ ,

$$\mathbf{U}(\mathbf{r}, t) = \frac{t^2}{2!} \mathbf{U}_2(\mathbf{r}) - \frac{t^4}{4!} \mathbf{U}_4(\mathbf{r}) + \dots, \quad (10)$$

$$\mathbf{U}_2(\mathbf{r}) = \frac{V}{m g(r)} \langle \delta(\mathbf{r} - \mathbf{r}_{21}) (\mathbf{F}_2 - \mathbf{F}_1) \rangle, \quad (11)$$

$$\begin{aligned} \mathbf{U}_4(\mathbf{r}) = & \frac{V}{m^2 g(r)} \sum_j \langle \delta(\mathbf{r} - \mathbf{r}_{21}) \{ (\mathbf{K}_{2j} - \mathbf{K}_{1j}) \times \mathbf{F}_j \\ & + k_B T (\mathbf{L}_{2jj} - \mathbf{L}_{1jj}) \} \rangle. \end{aligned} \quad (12)$$

With the definition of  $\mathbf{F}_i$  given in Eq. (4) and an identity due to an integration by parts, it is easy to prove that

$$\mathbf{U}_2(\mathbf{r}) = \frac{k_B T}{\mu g(r)} \nabla g(r) = -\frac{1}{\mu} \nabla w(r), \quad (13)$$

where  $\mu = m/2$ . Thus the  $t^2$  term in Eq. (10) is just the mean relative displacement in the CAA.

With the following identity, which also involves a suitable integration by parts [19],

$$\begin{aligned} & \langle \delta(\mathbf{r} - \mathbf{r}_{21}) \mathbf{K}_{ij} \cdot \mathbf{F}_j \rangle \\ & = k_B T \{ \delta_{j2} \nabla \cdot \langle \delta(\mathbf{r} - \mathbf{r}_{21}) \mathbf{K}_{i2} \rangle \\ & \quad - \delta_{j1} \nabla \cdot \langle \delta(\mathbf{r} - \mathbf{r}_{21}) \mathbf{K}_{i1} \rangle - \langle \delta(\mathbf{r} - \mathbf{r}_{21}) \mathbf{L}_{ijj} \rangle \}, \end{aligned} \quad (14)$$

where the symbol  $\delta_{ij}$  denotes the Kronecker  $\delta$  notation, and the contraction of divergence on a matrix is defined between the differential operator and the column index of the matrix, one can prove

$$\mathbf{U}_4(\mathbf{r}) = \frac{k_B T V}{m^2 g(r)} \nabla \cdot \langle \delta(\mathbf{r} - \mathbf{r}_{21}) (\mathbf{K}_{22} + \mathbf{K}_{11} - \mathbf{K}_{12} - \mathbf{K}_{21}) \rangle. \quad (15)$$

Then, by the definitions of  $\mathbf{K}_{22}$  and  $\mathbf{K}_{11}$  given in Eq. (7), we can separate  $U_4(\mathbf{r})$  into two terms  $\mathbf{U}_4^{(2)}(\mathbf{r})$  and  $\mathbf{U}_4^{(3)}(\mathbf{r})$ , where the former depends only on the pair with the initial separation at exactly  $\mathbf{r}$ , and the latter depends on three particles, two particles with the specified initial separation  $\mathbf{r}$  and a third one which can be any of the remaining particles in the system. Their expressions are given in the following:

$$\mathbf{U}_4^{(2)}(\mathbf{r}) = -\frac{k_B T V}{\mu^2 g(r)} \nabla \cdot \langle \delta(\mathbf{r} - \mathbf{r}_{21}) \mathbf{K}_{12} \rangle, \quad (16)$$

$$\mathbf{U}_4^{(3)}(\mathbf{r}) = -\frac{k_B T V}{m^2 g(r)} \nabla \cdot \sum_{j \neq 1,2} \langle \delta(\mathbf{r} - \mathbf{r}_{21}) (\mathbf{K}_{2j} + \mathbf{K}_{1j}) \rangle. \quad (17)$$

With the definition of  $\mathbf{K}_{12}$ , we can prove

$$\mathbf{U}_4^{(2)}(\mathbf{r}) = \frac{k_B T}{\mu^2 g(r)} \nabla \cdot (g(r) \mathbf{t}(\mathbf{r})). \quad (18)$$

Using the definition of the three-particle distribution function,

$$\rho^2 g_3(\mathbf{r}, \mathbf{r}') = \left\langle \sum_{i \neq j \neq 1} \delta(\mathbf{r} - \mathbf{r}_{i1}) \delta(\mathbf{r}' - \mathbf{r}_{j1}) \right\rangle, \quad (19)$$

$\mathbf{U}_4^{(3)}(\mathbf{r})$  can be expressed as

$$\mathbf{U}_4^{(3)}(\mathbf{r}) = \frac{\rho k_B T}{m^2 g(r)} \nabla \cdot \int d\mathbf{r}' g_3(\mathbf{r}, \mathbf{r}') (\mathbf{t}(\mathbf{r}') + \mathbf{t}(\mathbf{r}' - \mathbf{r})). \quad (20)$$

So far, this expression for  $\mathbf{U}_4^{(3)}(\mathbf{r})$  is exact. To facilitate the further calculation, we use the Kirkwood superposition approximation [20]

$$g_3(\mathbf{r}, \mathbf{r}') \approx g(r) g(r') g(|\mathbf{r} - \mathbf{r}'|). \quad (21)$$

After making this approximation, and then changing the integration variable of the second term in the integrand in Eq. (20),  $\mathbf{U}_4^{(3)}(\mathbf{r})$  is reduced to the following formula:

$$\mathbf{U}_4^{(3)}(\mathbf{r}) \approx \frac{2\rho k_B T}{m^2 g(r)} \nabla \cdot \int d\mathbf{r}' g(r) g(r') g(|\mathbf{r} - \mathbf{r}'|) \mathbf{t}(\mathbf{r}'). \quad (22)$$

From the above derivation, one can prove that the component of  $\mathbf{U}_4(\mathbf{r})$  perpendicular to the initial separation  $\mathbf{r}$  is zero, and the parallel component is given as the following:

$$U_4^{\parallel}(\mathbf{r}) \approx \frac{1}{\mu^2} \left[ -w'(r) \phi''(r) + k_B T \left[ \phi'''(r) + \frac{2}{r} \left( \phi''(r) - \frac{\phi'(r)}{r} \right) \right] \right] - \frac{2\rho}{m^2} (f_1 + f_2), \quad (23)$$

$$f_1 = w'(r) \int d\mathbf{r}' g(r') g(a) \left[ \frac{\phi'(r')}{r'} + \left( \phi''(r') - \frac{\phi'(r')}{r'} \right) (\hat{\mathbf{r}}' \cdot \hat{\mathbf{r}})^2 \right], \quad (24)$$

$$f_2 = \int d\mathbf{r}' g(r') g(a) w'(a) \left[ \frac{\phi'(r')}{r'} (\hat{\mathbf{a}} \cdot \hat{\mathbf{r}}) + \left( \phi''(r') - \frac{\phi'(r')}{r'} \right) (\hat{\mathbf{a}} \cdot \hat{\mathbf{r}}) (\hat{\mathbf{r}}' \cdot \hat{\mathbf{r}}) \right], \quad (25)$$

where  $\mathbf{a} = \mathbf{r} - \mathbf{r}'$  and  $\hat{\mathbf{a}}$  is the unit vector along  $\mathbf{a}$ .

In order to understand the above formula, we consider the relative motion of atomic pairs in a low-density (LD) fluid, in which two particles only interact with the potential  $\phi(r)$  and have randomly initial relative velocities satisfied with the Maxwell-Boltzmann distribution of temperature  $T$ . By using the method described above (integrating the equations of motion, iterating the displacements, and averaging out the initial velocities), up to the  $t^4$  order, the formula of the mean relative displacement in this low-density fluid is obtained, and given in the following:

$$U_{\text{LD}}^{\parallel}(r,t) = -\frac{t^2}{2\mu} \phi'(r) - \frac{t^4}{4!\mu^2} \left\{ -\phi'(r)\phi''(r) + k_B T \left( \phi'''(r) + \frac{2}{r} \left( \phi''(r) - \frac{\phi'(r)}{r} \right) \right) \right\} + \dots \quad (26)$$

Compared to the formula of the mean relative displacements in the high- and low-density limits, it is clear that up to the  $t^2$  order the relative motion of an atomic pair in a fluid is governed by the potential of mean force  $w(r)$ , rather than the direct potential  $\phi(r)$ . The potential of mean force between two particles in a fluid depends only on the static structures of the fluid, and has nothing to do with the motions of the remaining particles. In the  $t^4$  order, only partially affected by the potential of mean force owing to the evolution of the short-time dynamics to longer times, the relative motion of an atomic pair is, however, dominated by the direct potential  $\phi(r)$  and the two density-dependent  $f$  terms in Eq. (23), which give the lowest-order effect due to the relative motions between the pair and the remaining particles in the fluid.

### III. MOLECULAR-DYNAMICS SIMULATION AND COMPARISON

A system of 864 particles in a cubic box, interacting with the LJ potential

$$\phi(r) = 4\epsilon \left[ \left( \frac{\sigma}{r} \right)^{12} - \left( \frac{\sigma}{r} \right)^6 \right], \quad (27)$$

was simulated by the means of MD techniques with a velocity Verlet algorithm [21,22]. In our simulation, we have used the periodic boundary conditions and the minimum image convention. Also, the LJ potential is truncated at  $r_c = 3\sigma$ , and lifted by adding a term  $A(r/\sigma) + B$ , such that both the

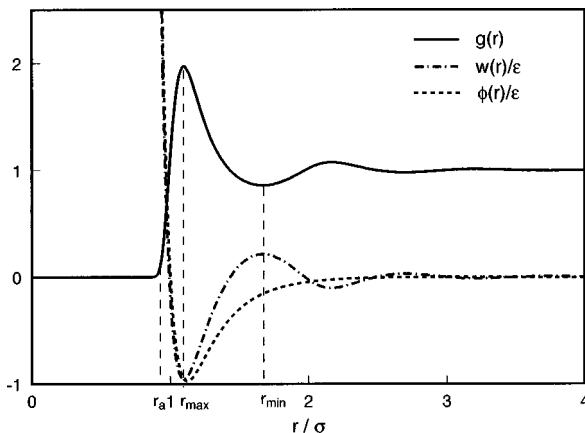


FIG. 1. The radial distribution function  $g(r)$  (solid line), the potential of the mean force  $w(r)$  (dot-dashed line), and the pair potential  $\phi(r)$  (dashed line) of the LJ fluid at  $\rho^* = 0.5$  and  $T^* = 1.41$ .

potential and the force at  $r_c$  are zero. The time unit used in this paper is  $t_0 = (m\sigma^2/\epsilon)^{1/2}$ , where  $\epsilon$  is the well depth of the potential and  $\sigma$  is the effective diameter of the particle. To obtain the thermal equilibrium, the system was propagated with a time step  $\Delta t = 0.01$ . After another equilibration run of 5000 steps, we changed the time step to be 0.001, and started to collect data. The chosen reduced density  $\rho^* \equiv \rho\sigma^3$  of the simulated fluid is 0.5, and the reduced temperature  $T^* \equiv k_B T/\epsilon$  is 1.41, which are the thermodynamic conditions studied by Saven and Skinner [7].

The radial distribution function  $g(r)$  was obtained directly from the simulation, and then the potential of the mean force  $w(r)$  was calculated according to its definition given in Sec. I. The calculated  $g(r)$  and  $w(r)$ , and the truncated-and-shifted LJ potential, are shown in Fig. 1. For  $r$  smaller than  $r_{\text{max}} \approx 1.1\sigma$ , which corresponds to the first maximum of  $g(r)$ , the function of  $w(r)$  is almost identical to the original pair potential; for  $r$  larger than  $r_{\text{max}}$ , the function is oscillatory, rather than monotonically increasing as in the LJ potential.

The mean-square displacement  $R(t) \equiv \langle |\mathbf{r}_1(t) - \mathbf{r}_1(0)|^2 \rangle$  of the single-particle motions in the LJ fluid we simulated is presented in Fig. 2. At  $t^* \equiv t/t_0 = 0.05, 0.1, 0.15, 0.2, 0.25,$

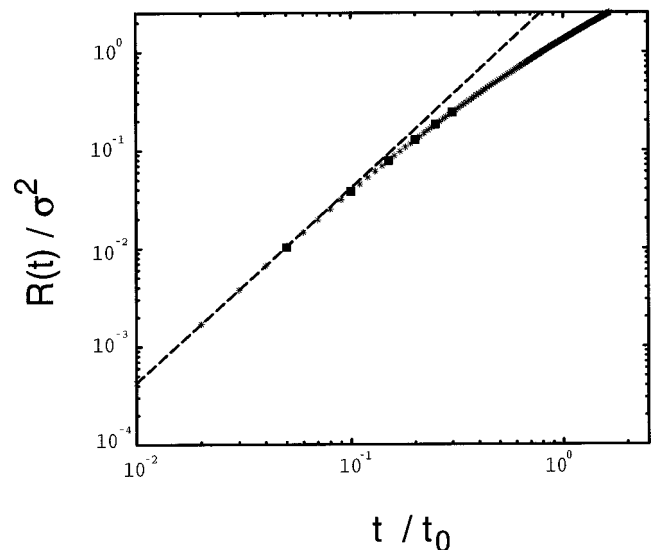


FIG. 2. The mean-square displacements  $R(t)$  of the single-particle motions vs time plotted on a log-log scale for the LJ fluid at  $\rho^* = 0.5$  and  $T^* = 1.41$ . The MD simulation data are represented by filled squares at  $t/t_0 = 0.05, 0.1, 0.15, 0.2, 0.25,$  and  $0.3$ , and by stars at other times. The dashed line is the short-time asymptotics of the simulation data.

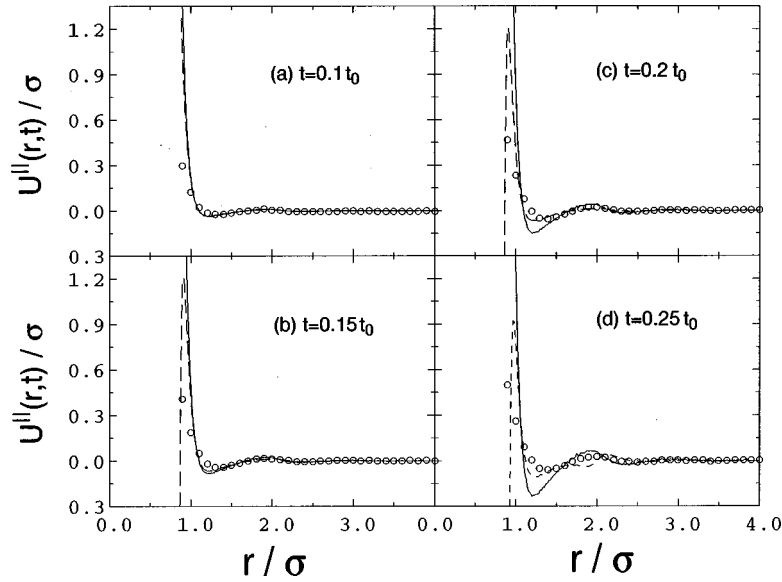


FIG. 3. The parallel components of the mean relative displacement as a function of the initial relative separation  $r$  at four different times. The open circles represent the simulation results. The solid and the dashed lines are the theoretical calculations by the CAA and the  $t^4$ -order approximation, respectively.

and 0.3, the simulation data of  $R(t)$  in Fig. 2 are manifested by filled squares. Generally speaking, for  $t^*$  less than 0.1,  $R(t)$  is proportional to  $t^2$ , and thus the single-particle motions within this time regime are ballistic. Since  $R(t)$  gradually deviates from its short-time asymptotics, the single-particle motions are no longer ballistic beyond  $t^* = 0.1$ . However, up to  $t^* = 0.3$ , the single-particle motions have yet to enter into the diffusion region.

In Fig. 3, we present the parallel component of the mean relative displacement as a function of the initial separation  $r$  at  $t^* = 0.1, 0.15, 0.2$ , and  $0.25$ , calculated by either the MD simulation, the CAA or the  $t^4$ -order approximation, through Eqs. (10), (13), (23), (24) and (25). The value of  $U^{\parallel}(r, t)$  obtained from MD calculation represents the average of the parallel relative displacement at time  $t$  for pairs of atoms with their initial separations between  $r - \delta r/2$  and  $r + \delta r/2$ . In this paper, we set  $\delta r$  to be  $0.05\sigma$ . We have checked the perpendicular component  $U^{\perp}(r, t)$ , which indeed has an average value of zero with a fluctuation less than 0.1%. In comparison, we found that at  $t^* = 0.1$  there is a good agreement between the simulation results and those of theoretical calculations for  $r$  larger than  $r_{\max}$ ; however, there is a large deviation for  $r$  less than  $r_{\max}$ . The smaller the initial separation of a pair, the larger the deviation. The deviation results from the fact that the force between two atoms of such a small separation is strong and changes rapidly. The short-time approximation for a mean relative displacement with  $r$  smaller than  $r_{\max}$ , therefore, breaks down even at  $t^* = 0.1$ . As time evolves, the region where the theoretical calculations deviate from the simulation results grows from the first shell of  $g(r)$  toward larger  $r$ . In general, results calculated with the  $t^4$ -order approximation indeed improve the predictions of the CAA. However, as  $t^*$  is larger than 0.15, the curve calculated by the  $t^4$ -order approximation has a sharp peak occurring at  $r$  smaller than  $r_{\max}$ . The occurrence of this sharp peak arises from the  $w'(r)\phi''(r)$  term in Eq. (23), which dominates over other terms, for  $w(r)$  is of the same order of magnitude as the pair potential  $\phi(r)$  in this region.

For two atoms in a fluid, the component of the averaged pair separation at time  $t$ , parallel to their initial separation  $\mathbf{r}$ , is given by  $d(r, t) \equiv r + U^{\parallel}(r, t)$ . In Fig. 4, we show the quantity  $d(r, t)$  as a function of time, with initial pair separations at  $r_a \approx 0.92\sigma, r_{\max}$ , and  $r_{\min} \approx 1.67\sigma$ , respectively, where  $r_{\min}$  corresponds to the first minimum of  $g(r)$  shown in Fig. 1. Since  $w'(r)$  at  $r_{\max}$  and  $r_{\min}$  are zero, both  $U^{\parallel}(r_{\max}, t)$  and  $U^{\parallel}(r_{\min}, t)$  in the CAA vanish at all times. However, the simulated results of  $d(r_{\max}, t)$  and  $d(r_{\min}, t)$  shown in Fig. 4 actually have small variations with time. Up to  $t^* = 0.3$ , the general trend of the variations is consistent with the theoretical predictions given by the  $t^4$ -order approximation of  $U^{\parallel}(r, t)$ . According to  $g(r)$ , a pair with initial separation at  $r_a$  can be recognized as two atoms being almost nearest neighbors in the fluid. For such a pair, the

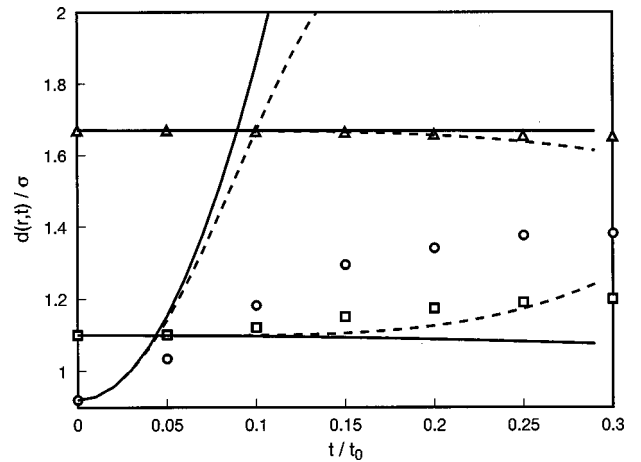


FIG. 4.  $d(r, t) \equiv r + U^{\parallel}(r, t)$  component of the pair separation parallel to the initial separation vector  $\mathbf{r}$ , as a function of time with the initial distance  $r \equiv |\mathbf{r}|$  of two atoms at  $0.92\sigma$  (open circles),  $1.1\sigma$  (open squares), and  $1.67\sigma$  (open triangles), respectively. The symbols are the simulation results. The solid and the dashed lines are the theoretical calculations by the CAA and the  $t^4$ -order approximation, respectively.

theoretical calculation of  $U^{\parallel}(r_a, t)$  given by either the CAA or the  $t^4$ -order approximation gives a good prediction only within a period less than  $0.05t_0$ , and breaks down as the separation of the pair approaches  $r_{\max}$ . By comparing the simulated results of  $d(r_a, t)$  and  $d(r_{\max}, t)$ , we give a physical picture of the relative motions of neighboring atoms in the LJ fluid we simulated. In general, for an atom in the fluid, its nearest neighbors are outwardly repelled very quickly due to the strong repulsive force from that atom. After penetrating through the first shell created by the central atom, those strongly repelled atoms keep moving outwardly in average within the time scale we study. On the other hand, the atoms originally staggering within the first shell tend to retain their separations with respect to the central atom within the time scales of ballistic motions, since the mean forces acting on them are almost zero. However, they are inclined to move outwardly, after those atoms originally attaching to the central atom pass through them.

One possible quantity to support this picture is the zeroth-angular moment of the  $G_2(\mathbf{r}, \mathbf{r}'; t)$  distribution [10], obtained by integrating over the solid angles  $\hat{\Omega}$  and  $\hat{\Omega}'$  corresponding to  $\mathbf{r}$  and  $\mathbf{r}'$ , respectively. The zeroth-angular moment of  $G_2$ , denoted by  $\gamma(r, r'; t)$ , is defined as

$$\gamma(r, r'; t) = \frac{1}{4\pi} \int d\hat{\Omega}' \int d\hat{\Omega} G_2(\mathbf{r}, \mathbf{r}'; t). \quad (28)$$

The normalization of this function is  $\int_0^\infty dr r^2 \gamma(r, r'; t) = 1$ . In Fig. 5, we present the  $\gamma(r, r'; t)$  functions with three initial pair separations as in Fig. 4 at five different times. In our calculation for  $\gamma(r, r'; t)$  from the simulation data, the resolutions  $\delta r$  and  $\delta r'$  for  $r$  and  $r'$ , respectively, were both set to be  $0.05\sigma$ . The  $\gamma(r, r'; t)$  function with the initial separation at  $r_a$  moves out radially more quickly than that with an initial separation at  $r_{\max}$ . At  $t^* = 0.1$ , the atoms which are originally at  $r_a$  have almost passed through  $r_{\max}$ ; however, those originally within the first shell of the central atom tend to remain there, with only part of them diffusing outwardly. On the other hand, the  $\gamma(r, r'; t)$  function with an initial separation at  $r_{\min}$  spreads out faster. At  $t^* = 0.25$ , some atoms originally at  $r_{\min}$  relative to the central atom have migrated into the first shell. Basically, the information about the relative motions of neighboring atoms provided by the  $\gamma(r, r'; t)$  function is consistent with the picture obtained above from analyzing the mean relative displacement.

It is well known that in the short-time limit the  $G_2(\mathbf{r}, \mathbf{r}'; t)$  distribution can be predicted well with the so-called short-time approximation [13], which is a Gaussian function of  $\mathbf{r}'$  with center at  $\mathbf{r} - t^2 \nabla w(r) / 2\mu$ . With the mean relative displacement  $\mathbf{U}(\mathbf{r}, t)$ , the  $G_2$  distribution beyond the short-time regime can be approximated with a Gaussian ansatz as given in the following:

$$G_2(\mathbf{r}, \mathbf{r}'; t) \approx \left( \frac{1}{2\pi A(t)} \right)^{3/2} \exp \left\{ - \frac{[\mathbf{r}' - \mathbf{r} - \mathbf{U}(\mathbf{r}, t)]^2}{2A(t)} \right\}, \quad (29)$$

where  $A(t) = k_B T t^2 / \mu$ . This Gaussian ansatz predicts the average center of  $G_2(\mathbf{r}, \mathbf{r}'; t)$  correctly, though not the spreading. With Eq. (29), the  $\gamma(r, r'; t)$  function can be calculated analytically to be:

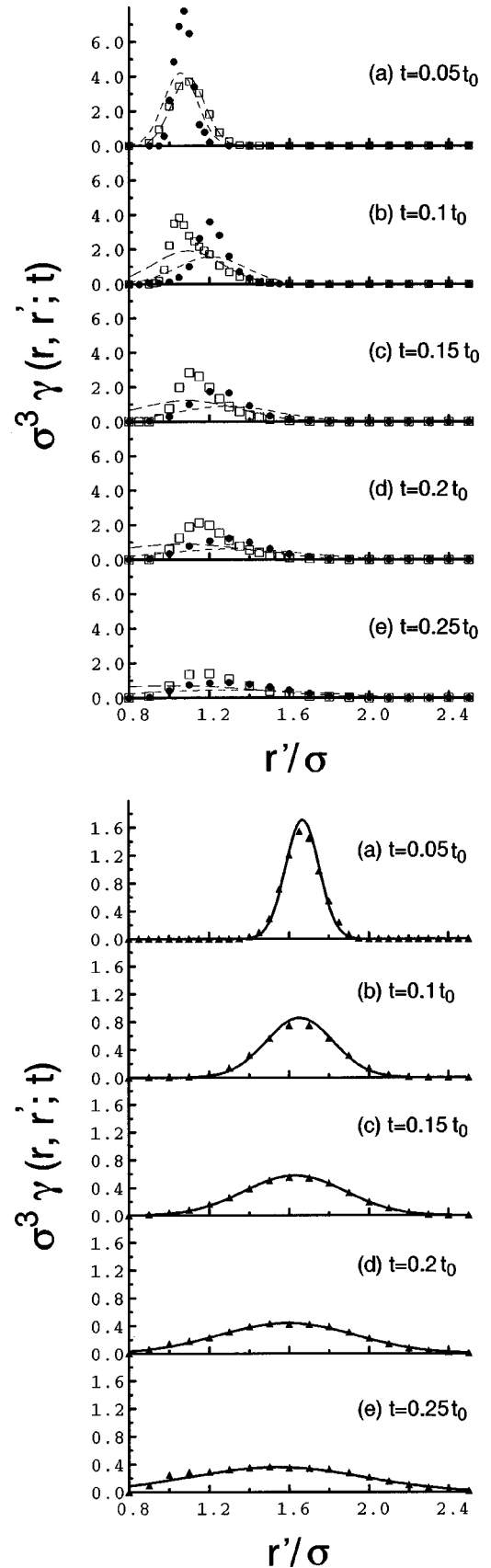


FIG. 5.  $\gamma(r, r'; t)$  as a function of  $r'$  at five different times with the initial pair separation  $r = 0.92\sigma$  (filled circles) and  $1.1\sigma$  (open squares) in (A), and  $r = 1.67\sigma$  (filled triangles) in (B). The solid and dashed lines are calculated with the Gaussian ansatz as described in the text. Note that the vertical scales in (A) and (B) are different.

$$\gamma(r, r'; t) \approx \frac{1}{(2\pi A(t))^{1/2} r' d(r, t)} \times \left\{ \exp\left[-\frac{(r' - d(r, t))^2}{2A(t)}\right] - \exp\left[-\frac{(r' + d(r, t))^2}{2A(t)}\right] \right\}, \quad (30)$$

where  $d(r, t)$  is the function shown in Fig. 4. With the simulated data of  $d(r, t)$ , a comparison of the  $\gamma(r, r'; t)$  function calculated with Eq. (30) and the simulated results is presented in Fig. 5 for the three initial pair separations considered above. Through this comparison, it seems that pairs of atoms with initial separations around  $r_{\min}$ , in general, undergo more freely mutual diffusion than those pairs with smaller initial separations. For  $r = r_a$  or  $r_{\max}$ , the spreading of the  $\gamma(r, r'; t)$  function predicted by Eq. (30) is too fast, for this Gaussian ansatz takes no account of effects due to collision with the core of the central atom.

#### IV. CONCLUSION

In this paper, we have defined the mean relative displacement of an atomic pair, which, we think, is an effective quantity to manifest the dynamics of atomic pairs in a fluid, especially for those pairs of neighboring atoms beyond the time regime described well in terms of the potential of mean force. The short-time expansion of the mean relative displacement has been derived exactly up to the  $t^4$  order. For a LJ fluid, the mean relative displacements calculated by either the CAA or the  $t^4$ -order approximation have been compared with the results obtained from the MD simulation.

In the short-time regime, within which single-particle motions are still recognized to be ballistic, the dynamics of atomic pairs in a fluid is well described by the CAA, and generally governed by the potential of mean force, which depends on the static structures of the fluid. Beyond this short-time regime, the relative motion of an atomic pair in a fluid is dominated by the direct pair potential between two atoms, and also influenced by the relative motions between the pair and the remaining particles.

By studying the relative motions of atomic pairs with initial separations either less than or at the distance corresponding to the first maximum of the radial distribution function, we have given a physical picture of the dynamics of atoms neighboring a central one. In the fluid we studied (low density and high temperature), the nearest neighbors to a given atom are repelled from the first shell created by that atom within the short-time regime mentioned above. Beyond this short-time regime, those atoms originally in the first shell diffuse away from that atom.

For LJ fluids with higher densities and lower temperatures [23] (at  $\rho^* = 0.85$  and  $T^* = 1.41$  and  $\rho^* = 0.85$  and  $T^* = 1.0$ ), the comparison between the mean relative displacements calculated with the  $t^4$ -order approximation and the simulation results are similar to the corresponding results presented in this paper, but the time regime for agreements is even smaller, since the time scale for ballistic motions in such a fluid is shorter. Roughly speaking, instead of penetrat-

ing through the first shell, the nearest neighbors of a given atom are trapped within the first shell before the shell spreads out.

Our results suggest that, rather than the potential of the mean force, a mean relative displacement analysis of the relative motions of atomic pairs in a fluid may provide an alternative to studying solvent effects on the transition frequency autocorrelation function. This will be the subject of a future work.

#### ACKNOWLEDGMENT

T.M.W. would like to acknowledge support from the National Science Council of Taiwan, R.O.C., under Grant No. NSC 88-2112-M-009-010.

#### APPENDIX

The total potential energy of a system of  $N$  particles in a configuration  $\mathbf{R}$  is  $V(\mathbf{R})$ . From the equations of motion, the displacement of the  $i$ th particle can be expressed as

$$\mathbf{u}_i(t) = \mathbf{v}_i t + \frac{1}{m} \int_0^t d\tau \int_0^\tau d\tau' \mathbf{F}_i(\tau'), \quad (A1)$$

where  $\mathbf{v}_i$  is the initial velocity of the  $i$ th particle.  $\mathbf{F}_i(\tau) \equiv -\nabla_i V(\mathbf{R})|_{\mathbf{R}=\mathbf{R}_\tau}$  is the total force on the  $i$ th particle at time  $\tau$ , and depends on the configuration of the system at time  $\tau$ ,  $\mathbf{R}_\tau \equiv (\mathbf{r}_1 + \mathbf{u}_1(\tau), \mathbf{r}_2 + \mathbf{u}_2(\tau), \dots, \mathbf{r}_N + \mathbf{u}_N(\tau))$ . As in the INM theory, the force  $\mathbf{F}_i(\tau)$  is expanded in the terms of the particle displacements from the initial configuration  $\mathbf{R}_0 \equiv (\mathbf{r}_1, \mathbf{r}_2, \dots, \mathbf{r}_N)$ . Up to the second order of displacements,

$$\mathbf{F}_i(\tau) = \mathbf{F}_i - \sum_j \mathbf{K}_{ij} \cdot \mathbf{u}_j(\tau) - \frac{1}{2} \sum_{j,k} \mathbf{u}_j(\tau) \cdot \mathbf{L}_{ijk} \cdot \mathbf{u}_k(\tau), \quad (A2)$$

where the expressions of  $\mathbf{F}_i$ ,  $\mathbf{K}_{ij}$ , and  $\mathbf{L}_{ijk}$  are given in Eqs. (4)–(6) in the text. After substituting Eq. (A2) into Eq. (A1), we obtain

$$\begin{aligned} \mathbf{u}_i(t) = & \mathbf{v}_i t + \frac{t^2}{2!m} \mathbf{F}_i - \frac{1}{m} \sum_j \mathbf{K}_{ij} \int_0^t d\tau \int_0^\tau d\tau' \mathbf{u}_j(\tau') \\ & - \frac{1}{2m} \sum_{j,k} \mathbf{L}_{ijk} \int_0^t d\tau \int_0^\tau d\tau' \mathbf{u}_j(\tau') \mathbf{u}_k(\tau') + \dots \end{aligned} \quad (A3)$$

After iterating the displacements  $\mathbf{u}_j(\tau')$  and  $\mathbf{u}_k(\tau')$  in Eq. (A3) with Eq. (A1), we may obtain the expansion of  $\mathbf{u}_i(t)$  in higher orders of time. The expansion of  $\mathbf{u}_i(t)$  up to the  $t^4$  order is given in Eq. (3) in the text.

- [1] P. F. Barbara and W. Jarzeba, *Adv. Photochem.* **15**, 1 (1990).
- [2] M. Maroncelli, *J. Mol. Liq.* **57**, 1 (1993).
- [3] M. L. Horng, J. A. Gardecki, A. Papazyan, and M. Maroncelli, *J. Phys. Chem.* **99**, 17 311 (1995).
- [4] R. M. Stratton and M. Maroncelli, *J. Phys. Chem.* **100**, 12 981 (1996).
- [5] B. M. Ladanyi and R. M. Stratton, *J. Phys. Chem.* **99**, 2502 (1995); **100**, 1266 (1996).
- [6] M. D. Stephens, J. G. Saven, and J. L. Skinner, *J. Chem. Phys.* **106**, 2129 (1997).
- [7] J. G. Saven and J. L. Skinner, *J. Chem. Phys.* **99**, 4391 (1993).
- [8] D. Chandler, *Introduction to Modern Statistical Mechanics* (Oxford University, Oxford, 1987), Chap. 7.
- [9] U. Balucani and R. Vallauri, *Physica A* **102**, 70 (1980); *Phys. Lett.* **76A**, 223 (1980); *Chem. Phys. Lett.* **74**, 75 (1980).
- [10] H. Posch, F. Vesely, and W. Steele, *Mol. Phys.* **44**, 241 (1981).
- [11] R. E. Larsen, E. F. David, G. Goodyear, and R. M. Stratton, *J. Chem. Phys.* **107**, 524 (1997).
- [12] A. M. Walsh and R. F. Loring, *Chem. Phys. Lett.* **186**, 77 (1991).
- [13] U. Balucani and M. Zoppi, *Dynamics of the Liquid State* (Oxford University Press, Oxford, 1994), Chap. 1.
- [14] S. W. Hann, *Phys. Rev. A* **20**, 2516 (1979).
- [15] I. Oppenheim and M. Bloom, *Can. J. Phys.* **39**, 845 (1961).
- [16] R. M. Stratton, *Acc. Chem. Res.* **28**, 201 (1995).
- [17] T. Keyes, *J. Phys. Chem. A* **101**, 2921 (1997).
- [18] T. M. Wu and R. F. Loring, *J. Chem. Phys.* **97**, 8568 (1992).
- [19] S. A. Egorov and J. L. Skinner, *J. Chem. Phys.* **105**, 7047 (1996).
- [20] J. G. Kirkwood, *J. Chem. Phys.* **3**, 300 (1935).
- [21] M. J. L. Sangster and M. Dixon, *Adv. Phys.* **25**, 247 (1976).
- [22] R. W. Hockney and J. W. Eastwood, *Computer Simulation Using Particles* (McGraw-Hill, New York, 1981).
- [23] S. L. Chang and T. M. Wu (unpublished).